

Development and Characterization of a Chronic Hepatitis B Murine Model With a Mutation in the START Codon of an HBV Polymerase

Lenka VANEKOVA^{1,2}, Marketa POLIDAROVA¹, Vilem CHARVAT^{1,3}, Zdenek VAVRINA^{1,2}, Vaclav VEVERKA^{1,2}, Gabriel BIRKUS¹, Andrea BRAZDOVA¹

¹Institute of Organic Chemistry and Biochemistry of the Czech Academy of Sciences, Prague, Czech Republic, ²Faculty of Science, Charles University, Prague, Czech Republic, ³First Faculty of Medicine, Charles University, Prague, Czech Republic

Received September 26, 2022

Accepted November 8, 2022

Epub Ahead of Print December 22, 2022

Summary

Chronic hepatitis B (CHB) is caused by the Hepatitis B virus (HBV) and affects millions of people worldwide. Developing an effective CHB therapy requires using *in vivo* screening methods, such as mouse models reflecting CHB based on hydrodynamic delivery of plasmid vectors containing a replication-competent HBV genome. However, long-term expression of HBV proteins is accompanied by production of progeny virions, thereby requiring a Biosafety Level (BSL) 3 animal facility. In the present study, we introduced a point mutation in the START codon of the HBV polymerase to develop a mouse model reflecting chronic hepatitis B infection without formation of viral progeny. We induced the mouse model by hydrodynamic injection of adeno-associated virus plasmid vector (pAAV) and minicircle plasmid (pMC) constructs into C57Bl/6 and C3H/HeN mouse strains, monitoring HBV antigens and antibodies in blood by enzyme-linked immunosorbent assay and analyzing liver expression of HBV core antigen by immunohistology. Persisting expression of viral antigens over 140 days (study endpoint) was observed only in the C3H/HeN mouse strain when using pAAV/1.2HBV-A and pMC/1.0HBV-D with pre-C and pre-S recombination sites. In addition, pAAV/1.2HBV-A in C3H/HeN sustained HBV core antigen positivity up to the study endpoint in C3H/HeN mice. Moreover, introducing the point mutation in the START codon of polymerase effectively prevented the formation of viral progeny. Our study establishes an accessible and affordable experimental paradigm for developing a robust mouse model reflecting CHB suitable for preclinical testing of anti-HBV therapeutics in a BSL2 animal facility.

Key words

Chronic hepatitis B murine model • HBsAg • HBeAg • pAAV system • Minicircle HBV

Corresponding author

A. Brazdova, Institute of Organic Chemistry and Biochemistry of the Czech Academy of Sciences, Flemingovo namesti 542/2, 160 00 Prague 6, Czech Republic. E-mail: andrea.brazdova@uochb.cas.cz

Introduction

Hepatitis B is a viral infection caused by the hepatitis B virus (HBV), small, enveloped DNA virus classified into ten genotypes (A-J) [1] that specifically target liver tissue. Approximately 95 % of adults suffering from acute HBV infection recover within 6 months by developing anti-HBV immunity. Those who do not develop immunity suffer from chronic hepatitis B (CHB), defined as the continuous blood circulation of a hepatitis B surface antigen (HBsAg) for more than six months. Moreover, up to 30 % of HBV-infected children under 5 years and up to 95 % of neonates develop CHB [2]. CHB may result in liver cirrhosis, steatosis, hepatocellular carcinoma, or adenoma [3-6].

The two available CHB therapies, interferon α -based therapy and nucleos(t)ide analogues, rarely result in the complete cure and often require life-long application [7], causing side effects [8]. Additionally, the long-term application of the first generation of nucleos(t)ide analogues (lamivudine and adefovir, among others) most

likely lead to viral resistance [9]. For these reasons, research and development of novel CHB therapeutics requires preclinical safety and efficacy validation.

Preclinical safety and efficacy research relies on animal models. However, the human HBV virus can only chronically infect humans and chimpanzees [10]. Alternatively, the human HBV-like family of viruses, which includes the woodchuck [11], domestic duck [12] and Beechey ground squirrel [13] subtypes, could be used as *in vivo* CHB models, but they require complying with stringent ethical, handling, and administrative procedures. Another difficulty with using these models is the lack of research tools for monitoring host-virus immune responses.

Murine CHB models, by contrast, are well established and much simpler to use. For example, transgenic HBV [14] and chimeric [15] mouse models are based on tail vein delivery of adeno-associated virus (AAV), whereas other models are induced by hydrodynamic injection (HDI [16]) of plasmid vectors carrying replication-competent DNA genome [17]. For these purposes, researchers usually resort to adeno-associated virus plasmid vector (pAAV) and covalently closed circular DNA plasmid produced by minicircle technology (pMC), which was primarily invented to address HBV cccDNA *in vivo* [17]. However, long-term HBV protein expression yields progeny virions, thereby requiring a Biosafety Level (BSL) 3 animal facility. Furthermore, sustained expression of viral markers in HDI-induced mouse models of CHB [18] depends on the selected mouse strain. In particular, major histocompatibility complex (MHC)-associated immune response to HBsAg affects model sustainability [19]. In terms of response to HBsAg, three different MHC genotypes are defined [19]: high (alleles H-2^{d,q}), intermediate (alleles H-2^a>H-2^b>H-2^k), and low/non-responders (alleles H-2^{s,f}).

To overcome these limitations, in this study, we aimed to develop and characterize a mouse model reflecting CHB induced by HDI delivery of HBV genome-encoding plasmids with a mutation in the START codon of the polymerase, which prevents the secretion of progeny virions by hepatocytes [17,20], in two different immunocompetent mouse strains, C57Bl/6 and C3H/HeN. In addition, we compared two different plasmid systems that encode HBV genomes of genotypes A and D, more specifically pAAV/1.2HBV genotype A (pAAV/1.2HBV-A) and D (pAAV/1.2HBV-D), pMC/1.0HBV genotype D with pre-C (pMC/1.0HBV-D-pre-C; encoding HBeAg [21]) and

pre-S (pMC/1.0HBV-D-pre-S; encoding envelope proteins [21]) residual recombination sites. Ultimately, the main purpose of this study was to create a mouse model that stably expresses HBsAg and HBeAg and is therefore suitable for robust preclinical testing of novel CHB therapeutics in a BSL2 animal facility.

Methods

Plasmids and mutagenesis

Two different types of plasmid constructs, a pAAV and minicircle, were used for mutated HBV genome delivery to establish a mouse model reflecting CHB. Plasmids carrying 1.2mer of HBV genome, genotype A (GenBank: AF305422.1, kindly provided [22]) or D (GenBank: MN645906.1, prepared in house) were inserted between inverted terminal repeats from AAV2 [23] (Fig. 1). Minicircle constructs [17,24] of 1.0mer of HBV genotype D genome with a residual recombination site in the pre-S or pre-C region were prepared according to Yan *et al.* [17] and to Wang *et al.* [25]. A point mutation T2308C [17] of the polymerase START codon was introduced to prevent the formation of HBV virions. The pAAV plasmids were isolated using the Nucleobond Xtra Midi EF kit (Macherey Nagel) according to the manufacturer's instructions. The minicircles were prepared from pre-MC plasmids, also according to the manufacturer's instructions (MC-Easy Minicircle DNA Production Kit, BioCat), and isolated using the Nucleobond Xtra Maxi EF kit (Macherey Nagel). The endotoxin level in DNA was quantified using HEK-Blue™ LPS Detection Kit 2 (InvivoGen) in HEK-Blue™hTLR4 cells (InvivoGen), according to the manufacturer's instructions. Plasmid integrity, quality and functionality were tested (data not shown, plasmids were tested *in vitro* using HepG2-NTCP transfection system and the levels of HB-Ag secreted into media were tested; *in vivo* viral progeny absence was verified in mouse plasma using qPCR).

In vivo mouse model reflecting CHB

All animal procedures were approved by institutional and national committees for the care and use of laboratory animals (CAS 77/2018, MSMT 29416/2020-7, Czech Republic). All animal experiments were performed in accordance with European Guidelines on Laboratory Animal Care. The HDI model was induced in male C3H/HeN and C57Bl/6 mice (aged 4-6 weeks [26], purchased from the Charles River Laboratories) by

tail vein injection of 10 µg of endotoxin free pAAV/1.2HBV plasmid DNA [27] or 5 g of endotoxin free pMC/1.0HBV DNA [17] in a tempered saline solution within 5-8 s in a volume equal to 10 % of the mouse body weight [28]. Blood samples were collected into lithium-heparin tubes (Microvette CB 300, Sarstedt) every 1-3 weeks for up to 20 weeks. The mice were housed in specific, pathogen-free conditions in an individually ventilated cage-system with food and water *ad libitum* under controlled temperature and light settings and monitored weekly for general appearance (weight, fur ruffling, and mobility/activity).

HBV antigen secretion analysis

The blood levels of the HBV surface, the HBV envelope-relevant antigens (HBsAg and HBeAg), and the antibody against HBsAg (HBsAb) were determined using an ELISA kit (Bioneovan Co., Ltd.) according to the adapted manufacturer's recommendations. The absorbance was measured on a Spark reader (Tecan). The internally established positivity threshold was determined as 5× the mean of HDI controls for HB-Ag markers and as 3× the mean of HDI controls for the HBsAb marker.

HBcAg immunohistochemistry (IHC)

The liver was preserved in 4 % paraformaldehyde (Sigma-Aldrich) for 24-48 h and kept in 70 % ethanol (Penta s.r.o.) until analysis. Liver tissue was stained with polyclonal rabbit anti-HBcAg antibody (DAKO-Agilent). HBcAg positivity was defined as a percentage of positive cells in the entire sample.

Statistical analysis

All statistical tests of experimental data were performed in GraphPad Prism software (La Jolla, CA, version 8.0.1). Data were presented as Kaplan-Meier curves or mean ± standard error of mean (SEM). HB-Ag positivity was analyzed using the Log-rank comparison test. The normality of distributions was tested using the Shapiro-Wilk test. The trend of HB-Ag levels over time was assessed according to the Spearman's rank correlation test, and the HB-Ag terminal levels was analyzed using the Mann-Whitney U-test.

Results

T2308C mutation of the polymerase START codon does not affect *in vitro* plasmid functionality

Both pAAV [22] and pMC [17,24] plasmids carrying the replication-competent HBV DNA genome

(henceforth referred to as wild type, wt) or the HBV DNA genome with a mutation of the START codon of the polymerase (T2308C [17], Fig. 1) were produced. The *in vitro/in vivo* quality, purity, and functionality were tested (data not shown). The T2308C point mutation was effectively introduced and had a non-significant effect on the *in vitro* expression of HB-Ag when compared to the wt plasmid using an *in vitro* HepG2-NTCP infection system [29]. The absence of HBV virions using plasmids with a point mutation in the START codon of polymerase was verified in mouse plasma by quantitative polymerase chain reaction (qPCR), showing that HBV DNA was below the limit of detection.

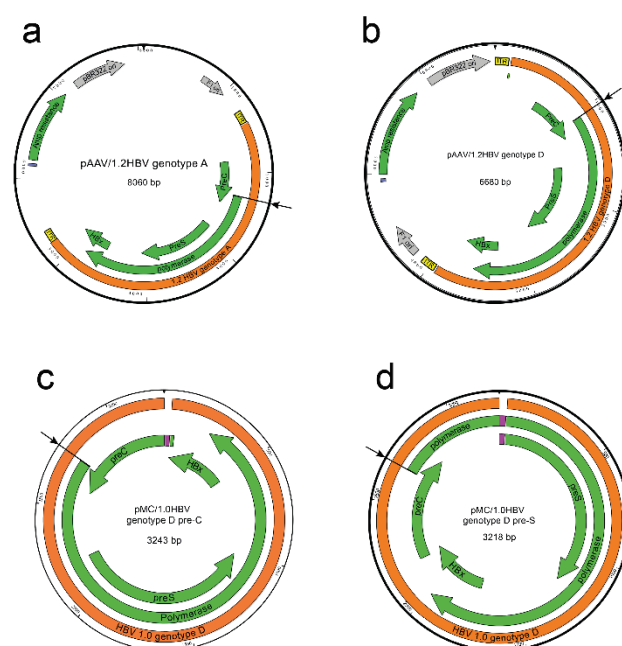


Fig. 1. Plasmid maps: pAAV/1.2HBV-A (a) and D (b), pMC/1.0HBV-D-pre-C (c) and pre-S (d); mutation T2308C [17] eliminating the START codon of the HBV polymerase pointed as an arrow; the orange represents the HBV sequence; green represents open reading frames encoding the polymerase, HBx = HBV X protein, pre-C region encoding HBeAg and HBcAg, pre-S domain encoding 3 forms of HBsAg; grey represents the bacterial origin of replication; yellow represents inverted terminal repeats from AAV2 virus; blue represents promoter, and purple represents the ATT recombination site (resulting from a minicircle preparation from the parental plasmid [17]).

The *in vivo* mouse model was hydrodynamically induced *via* tail vein (Fig. 2a). We compared PBS to a physiologic solution. The physiologic solution increased the HDI survival rate up to 100 % (data not shown) in contrast to 20 % using commercially available PBS (without calcium and magnesium chloride, Sigma Aldrich, Cat. No. D8537).

C57Bl/6 and C3H/HeN male mice were

hydrodynamically injected with either 10 μg of pAAV/1.2HBV or 5 μg of pMC/1.0HBV plasmids with the point mutation T2308C (Fig. 2a). These doses were previously described as optimal when using nonmutated wild type (wt) plasmids for long-term HBV persistence without HBsAg seroconversion [17,27]. The models were

evaluated based on the HB-Ag levels, and sustainability was determined by seroconversion in the presence of anti-HBsAg antibodies (HBsAb) in blood (Fig. 2, Fig. 3, Fig. 4) and further confirmed by HBcAg expression in the liver (Fig. 5).

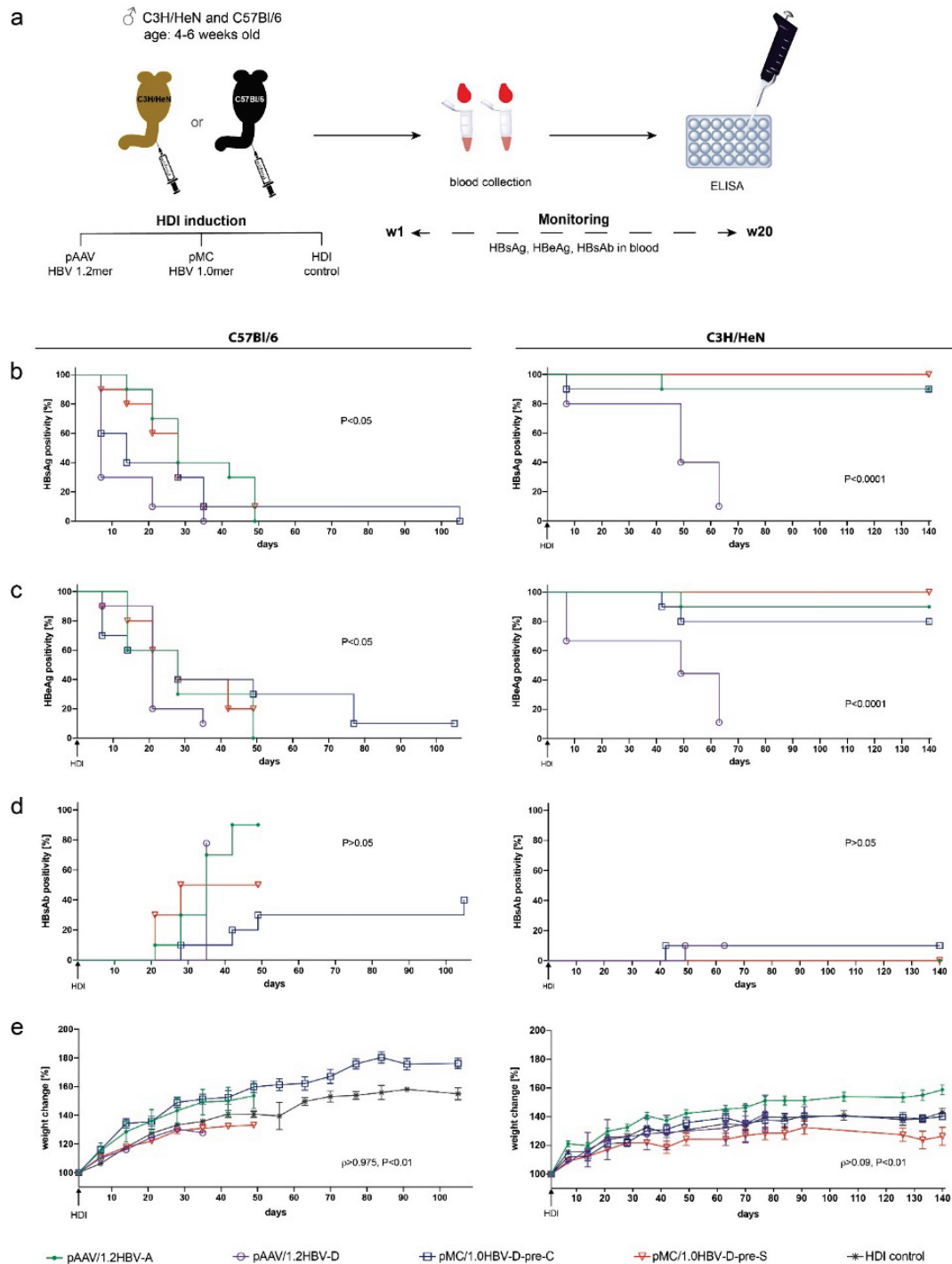


Fig. 2. CHB *in vivo* model establishment and characterization in C57Bl/6 and C3H/HeN mice: (a) scheme of the experiment and continuous monitoring of HBsAg (b), HBeAg (c) and HBsAb (d) blood levels; the positivity proportions of all induction systems (pAAV/1.2HBV-A and D, pMC/1.0HBV-D-pre-C and pre-S) are shown as Kaplan-Meier curves and compared using the Log-rank test. (b, c, d) n=5-20 mice/group. (e) Weight as stratified by induction system groups for both mouse strains, data were analyzed using Spearman correlation test, ρ expressing Spearman's rank correlation coefficient. Data expressed as mean value per group \pm SEM. n=5-20 mice/group.

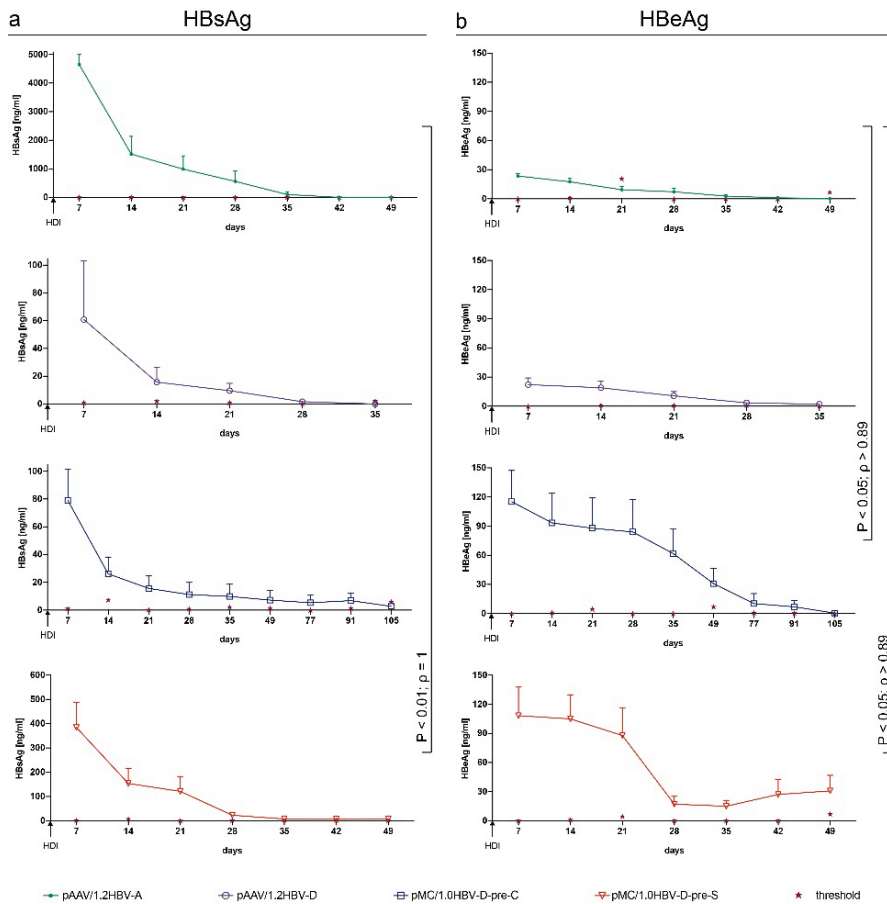


Fig. 3. HBV marker levels in CB7Bl/6 mice: HBsAg (a) and HBeAg (b) were monitored in animals hydrodynamically injected with plasmid constructs. Data were compared using the Spearman correlation test; unless otherwise stated, $P > 0.05$, ρ expressing Spearman's rank correlation coefficient. Data were expressed as mean \pm SEM per group. (a, b) $n = 5-20$ mice/group.

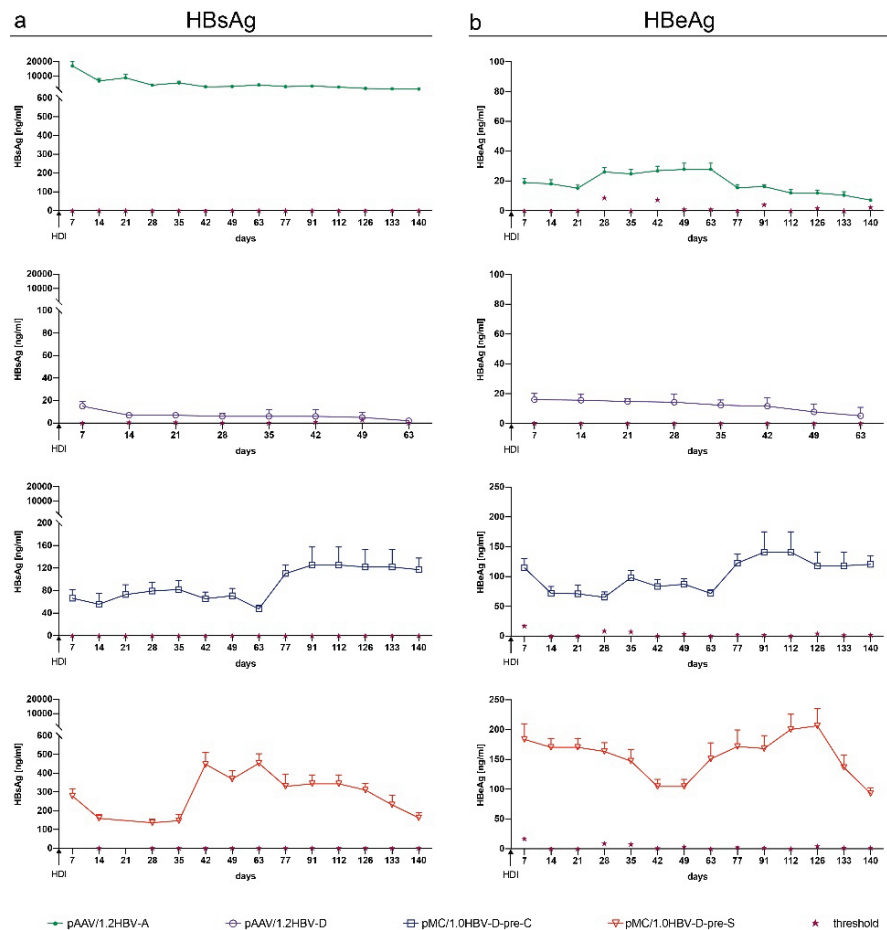


Fig. 4. HBV marker levels in C3H/HeN mice: HBsAg (a) and HBeAg (b) were monitored in animals hydrodynamically injected with plasmids. Data were compared using the Spearman correlation test (all data were non-significant (ns) = $P > 0.05$). Data were expressed as mean \pm SEM per group. (a, b) $n = 5-20$ mice/group.

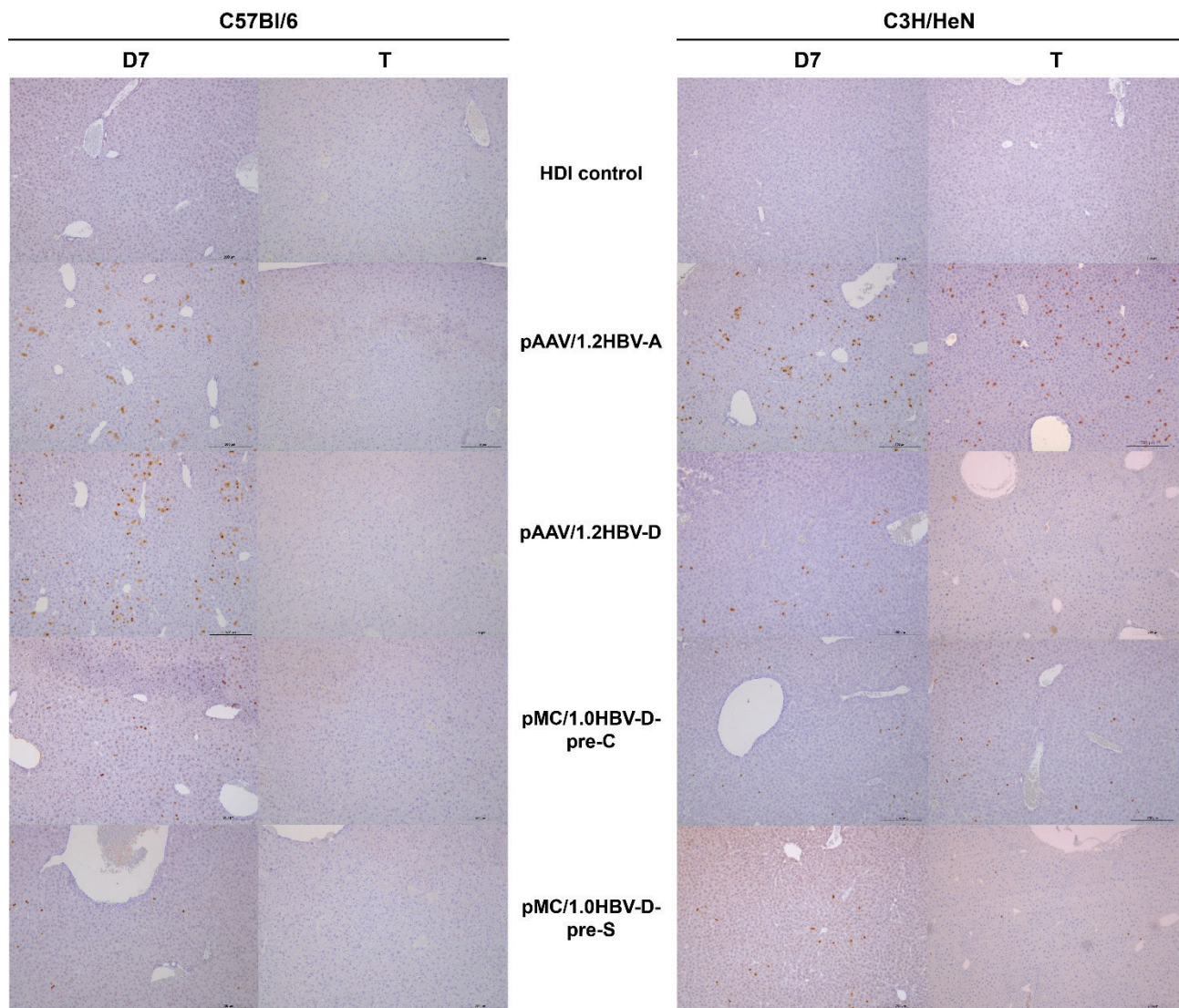


Fig. 5. HBeAg expression in liver sections of C57Bl/6 and C3H/HeN mice detected by immunohistochemistry: HBeAg detected on day 7 (D7) post HDI and at the terminal point of the experiment (T; C57Bl/6: D35 pAAV/1.2HBV-D, D49 pAAV/1.2HBV-A and pMC/1.0HBV-D-pre-S, D105 pMC/1.0HBV-D-pre-C; C3H/HeN: D62 pAAV/1.2HBV-D, D140 pAAV/1.2HBV-A, pMC/1.0HBV-D-pre-C and pMC/1.0HBV-D-pre-S); representative results of HBeAg (brown spots) per induction system group.

Hydrodynamic injection of pAAV/1.2HBV and pMC/1.0HBV with a START codon mutation of the polymerase into C57Bl/6 mice results only in transient expression of viral proteins

In C57Bl/6 mice, the blood levels of HBsAg and HBeAg started decreasing within the first week post HDI. Mice injected with pAAV/1.2HBV-D showed a rapid loss of HBsAg (no animal was positive by D35, Fig. 2b). In addition, 80 % of animals had cleared HBeAg within D21 post HDI (Fig. 2c), and 80 % of mice were positive for HBsAb (Fig. 2d) by D35.

Due to this rapid clearance of HB-Ag (Fig. 2b, c) and to the very low HBV persistence rate observed when using pAAV/1.2HBV-D, the minicircle construct [17] of genotype D was prepared. pMC/1.0HBV-D-pre-C

injection into C57Bl/6 mice resulted in a relatively fast clearance of HBsAg (only 10 % positive mice by D35, Fig. 2b) and in lower HBsAg levels (Fig. 3a) than when injecting the pAAV/1.2HBV-D (Fig. 3a), albeit with 10 % positivity up to D105 (Fig. 2b). HBeAg positivity decreased from 70 % (D7) to 30 % (D49) and finally up to 10 % (D77) and sustained to the terminal point of experiment (D105, Fig. 2c), with more than 10× higher HBeAg levels than those observed in animals injected with pAAV/1.2HBV-D (Fig. 3b). HBsAb were detected within 4 weeks post HDI, and by the end of the study, up to 40 % animals had seroconverted (D105, Fig. 2d).

By D21, mice injected with pMC/1.0HBV-D-pre-S showed a mild decrease of HBsAg-related positivity (10-20 % loss every week, Fig. 2b) with mean

plasma HBsAg values >100 ng/ml (Fig. 3a). However, HBsAg-related positivity rapidly dropped to 10 % until D35 (Fig. 2b), while HBeAg positivity decreased gradually to 20 % until D49 (Fig. 2c), with HBeAg plasma levels similar to but less consistent than those measured when injecting pMC/1.0HBV-D-pre-C (Fig. 3b). HBsAb related positivity increased up to 50 % until D28 (Fig. 2d).

Even though C57Bl/6 mice injected with pAAV/1.2HBV-A showed the most promising results (with a mean peak HBsAg concentration of 4500 ng/ml, which was considerably higher than those of other induction systems, Fig. 3a), all animals showed total loss of HBsAg and HBeAg by D49 (Fig. 2b, Fig. 2c, Fig. 3a, Fig. 3b), while HBsAg seroconversion rapidly increased from 10 % (D21, Fig. 2d) to 90 % within 2-3 weeks post HDI (Fig. 2d). Based on our results, when using pAAV/1.2HBV-A, we also tested pMC/1.0HBV-A-pre-C in CB7Bl/6 mice. However, we observed only acute expression of HB-Ag (total loss of HB-Ag by D28), as in pAAV/1.2HBV-D (data not shown).

Hydrodynamic injection of pAAV/1.2HBV-A with a mutated polymerase START codon into C3H/HeN mice leads to a persistent expression of viral proteins

HDI injection of the plasmids into the C3H/HeN mouse strain led to a much more consistent and sustainable expression of viral proteins. More than 80 % of animals remained HB-Ag-positive up to the end of the study (D140, the study endpoint) when using pMC/1.0HBV-D-pre-C, pMC/1.0HBV-D-pre-S, and pAAV/1.2HBV-A (Fig. 2b, c, Fig. 4a, b). However, pAAV/1.2HBV-D induced only a transient expression of viral proteins, albeit for a longer period time in C3H/HeN mouse strain than in C57Bl/6 mice (Fig. 2b, c). On D7 after HDI, 70-80 % of animals were HB-Ag-positive, but this positivity had dropped to 10 % by D62 (Fig. 2b, c). Furthermore, only 10 % of the mice injected with pAAV/1.2HBV-D developed HBsAb (Fig. 2d). In contrast to pAAV/1.2HBV-D, pAAV/1.2HBV-A, pMC/1.0HBV-D-pre-C and pMC/1.0HBV-D-pre-S showed a similar chronic expression of viral antigens (nonsignificant, Fig. 2b, c). Interestingly, pMC/1.0HBV-A-pre-C showed only a transient expression of viral proteins (total loss of HB-Ag by D49, data not shown) similar to that of pAAV/1.2HBV-D.

We also observed differences in the average values of detected HB-Ag between all constructs. The minicircle constructs using genotype D had low HBsAg levels (pMC/1.0HBV-D-pre-C <200 ng/ml,

pMC/1.0HBV-D-pre-S <500 ng/ml, Fig. 4a), while pAAV/1.2HBV-A had >40× higher average values of HBsAg (<20000 ng/ml, Fig. 4a). The endpoint HBsAg values were significantly different between pAAV/1.2HBV-A and pMC/1.0HBV-D-pre-S and pre-C, but the plasma endpoint levels of HBeAg were significantly higher when using the minicircle constructs (120-200 ng/ml, Fig. 4b) than when using pAAV/1.2HBV-A (<30 ng/ml, Fig. 4b).

HBcAg was detected only in C3H/HeN mice hydrodynamically injected with both pAAV/1.2HBV and pMC/1.0HBV with a mutation of polymerase at the terminal point of the experiment

The expression of HBcAg in mouse hepatocytes was determined by immunohistochemical analysis of liver tissue on D7 [27] post HDI and at the terminal point of the experiment. In C57Bl/6 mice, IHC confirmed the presence of HBcAg positive cells on D7 post HDI regardless of HBV construct, with pAAV/1.2HBV-A resulting in 20-25 % HBcAg-positive cells; pAAV/1.2HBV-D, 10-25 % HBcAg-positive cells; and both pMC/1.0HBV-D-pre-C and pre-S, <10 % HBcAg-positive cells (Fig. 5). However, not a single liver tissue showed the HBcAg positivity at the end of the study (Fig. 5). C3H/HeN mice showed 20-25 % HBcAg-positive hepatocytes for pAAV/1.2HBV-A and 10-15 % HBcAg-positive hepatocytes for genotype D on D7 post HDI regardless of plasmid induction system. The HBcAg positivity of the genotype D of both systems, pAAV and pMC, decreased to <10 % of positive cells at the terminal point of the experiment. Conversely, HBcAg positivity remained unchanged when using pAAV/1.2HBV-A in C3H/HeN mice. The positive hepatocytes were unevenly distributed in most samples. Mice injected only with physiologic solution (HDI control, Fig. 5) were HBcAg-negative throughout the experiment regardless of induction construct.

Regardless of mouse strain or HBV genotype, HBV transduction was latent. In both mouse strains, none of the induction systems affected physiology, as confirmed by the absence of weight changes (Fig. 2e). The mice were also monitored weekly for general appearance (fur ruffling, mobility, and activity), showing no pathologic changes.

Discussion

Our immunocompetent CHB mouse model induced by HDI delivery of plasmid vector [18] stably

expresses the viral markers HBsAg and HBeAg for 20 weeks without viral progeny. As such, this model is suitable for robust preclinical safety and efficacy testing of novel CHB therapeutics. Although research on CHB mouse models has recently led to the development of several other murine models [18], such as transgenic [14] and chimeric [15] mouse models, as well as models based on tail vein delivery of viral vectors carrying HBV DNA genome [16], they all have some limitations, including requiring BSL3 animal facilities [30]. To overcome these limitations, we first compared two most commonly used vehicles for HDI injection, physiologic solution [27] and PBS [22] particularly regarding their formulation in terms of acid-base balance disruption (e.g. calcium, magnesium and/or potassium chloride). Despite the broad use of PBS as a vehicle for *in vivo* transfection (e.g. targeted [31] and pressurized [22]), the physiologic solution dramatically positively affected HDI survival. We also used pAAV [22,27] and pMC [17] plasmid vectors carrying 1.2mer and 1.0mer HBV DNA genome respectively (genotype A and D) dosed as previously described [17,27] with a T2308C [17] point mutation of the START codon of the polymerase to prevent the production of infectious HBV progeny [17], as confirmed using all induction systems, without affecting HBV transcription and antigen expression. Therefore, this point mutation allows us to operate in a BSL2 animal facility.

We chose two mouse strains of different MHC classes with different immune responses to HBsAg that prevent spontaneous healing [19] namely C57Bl/6 and C3H/HeN, to comparatively assess HB-Ag persistence. HBsAg is considered a general marker of HBV in both mouse and human plasma [32], regardless of acute or chronic infection. Unlike HBsAg, HBsAb indicates the generation of specific immunity leading to host recovery. Since HBsAb production is affected by S region-encoding MHC class III complement components, including C⁴ and C² [19], we tested mouse strains from an intermediate MHC genotype group with different haplotypes, i.e. C57Bl/6 (haplotype b) and C3H/HeN (haplotype k).

In line with Peng *et al.* [20], we demonstrated that the C57Bl/6 mouse strain bearing the S^b region with a sufficient response to HBsAg leads to HB-Ag clearance (Fig. 2b, Fig. 3), as observed across all induction systems, resulting in only an acute HBV model, unlike other studies [22,27], where HB-Ag expression persisted for more than 6 months when using replication-competent

HBV genome in C57Bl/6 mice. This result could be explained by differences in positivity threshold setting and in animals from different vendors. Moreover, the introduced point mutation may also partly account for this discrepancy between studies.

The C3H/HeN mouse strain markedly increased and sustained viral antigen expression, as also demonstrated by Peng *et al.* and Yan *et al.* [17,20] using non-mutated pAAV/1.2HBV and pMC/1.0HBV. Based on humoral immunity in C3H/HeN mice (S^k region), we assume that the insufficient HBsAg response reflects its persisting levels and the low levels of seroconversion (Fig. 2b, d, Fig. 4a).

We confirmed the persistence and clearance of viral markers by immunohistochemical analysis of HBeAg in liver tissue, showing HBV clearance through the decreased HBsAg and HBeAg positivity in C57Bl/6 mice over time (Fig. 2b, c, Fig. 3a, b) along with increased HBsAb levels (Fig. 2d) matching the decreased HBeAg positivity. These results also corroborate Li *et al.* [27], who quantified HBeAg-levels in C57Bl/6 mice after using pAAV/1.2HBV. Unlike them [27], nevertheless, we detected lower HBcAg positivity on D7 after HDI and no HBcAg positivity at the terminal point of the experiment (D49). A possible reason for this difference may be the point mutation of the polymerase START codon. HBcAg positivity was sustained at a max. of 25 % using pAAV/1.2HBV-A in C3H/HeN mice, matching the persisting levels of HBsAg expression (Fig. 2b, Fig. 4a). Our results using both mouse strains correlate with the findings of Peng *et al.* [20] who reported that C3H/HeN mice were superior to C57Bl/6 mice in HBcAg positivity when using a non-mutated pAAV/1.2HBV induction system.

Considering the plasma levels of the viral markers, the efficacy of the induction systems in both C57Bl/6 and C3H/HeN mice was reflected as a trend of pAAV/1.2HBV-A \geq pMC/1.0HBV-D-pre-S $>$ pMC/1.0HBV-D-pre-C \gg pAAV/1.2HBV-D. Unlike all induction plasmids in C57Bl/6 mice and pAAV/1.2HBV-D in C3H/HeN mice, HB-Ag positivity persisted until the terminal point of the experiment (D140) using pAAV/1.2HBV-A and both minicircle constructs in C3H/HeN mice. In contrast to genotype A, genotype D has a 33-nucleotide deletion in the N terminus of the PreS1 region [33]. This deletion changes the ratio of the three S antigen forms and affects their secretion [34], which may thus explain why the HBsAg-levels were significantly lower in mice induced with genotype D.

The differences in HBeAg-levels among plasmids in both mouse strains might be associated with the use of different induction systems. Unlike pAAV, the pMC HDI induction system was primarily developed to address cccDNA *in vivo* [17]. As previously described [35], HBeAg secretion and cccDNA formation may be correlated; if so, significantly higher HBeAg levels should be found when using minicircle constructs. However, the point mutation of the START codon of the polymerase adversely affected the viral replication cycle. Consequently, the formation of new cccDNAs [36] resulted in similar if not lower HBeAg-levels during the experiment. Nevertheless, HBeAg persistence is variable even among CHB patients and thus not a definitive CHB marker [37].

In conclusion, the C3H/HeN mouse strain is more suitable than C57Bl/6 for developing a long-term *in vivo* model reflecting CHB. Based on the pAAV/1.2HBV-A-associated HBsAg-levels, in contrast to pMC/1.0HBV-D-pre-S-associated HBsAg-levels, we believe that the pAAV induction system provides more suitable experimental paradigm for various immunopathology studies aimed at assessing the efficacy

and safety of novel therapeutic approaches requiring robust yet simple *in vivo* testing. Notwithstanding previously published mouse models, we firmly believe that the persistence of HBsAg levels in our mouse model using pAAV/1.2HBV-A with a T2308C point mutation in the polymerase START codon could last much longer than 20 weeks. Thanks to the T2308C [17] point mutation of the polymerase START codon and the resulting lack of virion progeny; such *in vivo* testing can be routinely performed in a BSL2 animal facility. Our model provides several advantages, including its accessibility, convenience, and affordability.

Conflict of Interest

There is no conflict of interest.

Acknowledgements

This research was funded by the OP RDE Project entitled “Chemical biology for drugging undruggable targets” Chem-BioDrug. No. CZ.02.1.01/0.0/0.0/16_019/0000729. The authors thank Dr. Carlos V. Melo for editing the manuscript.

References

1. Sunbul M. Hepatitis B virus genotypes: Global distribution and clinical importance. *World J Gastroenterol* 2014;20:5427-5434. <https://doi.org/10.3748/wjg.v20.i18.5427>
2. World Health Organization. Global Hepatitis Report 2017;2017.
3. Krajden M, McNabb G, Petric M. The laboratory diagnosis of hepatitis B virus. *Can J Infect Dis Med Microbiol* 2005;16:65-72. <https://doi.org/10.1155/2005/450574>
4. Ha HL, Shin HJ, Feitelson MA, Yu DY. Oxidative stress and antioxidants in hepatic pathogenesis. *World J Gastroenterol* 2010;16:6035-6043. <https://doi.org/10.3748/wjg.v16.i48.6035>
5. Liu L, Yang F. Application of modified mesenchymal stem cells transplantation in the treatment of liver injury. *Physiol Res* 2021;70:327-343. <https://doi.org/10.33549/physiolres.934623>
6. Farghali H, Kgalalelo Kemelo M, Wojnarová L, Kutinová Canová N. In vitro and in vivo experimental hepatotoxic models in liver research: applications to the assessment of potential hepatoprotective drugs. *Physiol Res* 2016;65(Suppl 4):S417-S425. <https://doi.org/10.33549/physiolres.933506>
7. Akbar SMF, Al Mahtab M, Aguilar JC, Yoshida O, Khan S, Penton E, Gerardo GN, Hiasa Y. The Safety and Efficacy of a Therapeutic Vaccine for Chronic Hepatitis B: A Follow-Up Study of Phase III Clinical Trial. *Vaccines (Basel)* 2022;10:45. <https://doi.org/10.3390/vaccines10010045>
8. Leowattana W, Leowattana T. Chronic hepatitis B: New potential therapeutic drugs target. *World J Virol* 2022;11:57. <https://doi.org/10.5501/wjv.v11.i1.57>
9. Liu T, Sun Q, Gu J, Cen S, Zhang Q. Characterization of the tenofovir resistance-associated mutations in the hepatitis B virus isolates across genotypes A to D. *Antiviral Res* 2022;203:105348. <https://doi.org/10.1016/j.antiviral.2022.105348>
10. Wieland SF. The chimpanzee model for hepatitis B virus infection. *Cold Spring Harb Perspect Med* 2015;5:a021469. <https://doi.org/10.1101/cshperspect.a021469>

11. Summers J, Smolec JM, Snyder R. A virus similar to human hepatitis B virus associated with hepatitis and hepatoma in woodchucks. *Proc Natl Acad Sci U S A* 1978;75:4533. <https://doi.org/10.1073/pnas.75.9.4533>
12. Mason WS, Seal G, Summers J. Virus of Pekin ducks with structural and biological relatedness to human hepatitis B virus. *J Virol* 1980;36:829. <https://doi.org/10.1128/jvi.36.3.829-836.1980>
13. Marion PL, Oshiro LS, Regnery DC, Scullard GH, Robinson WS. A virus in Beechey ground squirrels that is related to hepatitis B virus of humans. *Proc Natl Acad Sci U S A* 1980;77:2941. <https://doi.org/10.1073/pnas.77.5.2941>
14. Guidotti LG, Matzke B, Schaller H, Chisari FV. High-level hepatitis B virus replication in transgenic mice. *J Virol* 1995;69:6158-6169. <https://doi.org/10.1128/jvi.69.10.6158-6169.1995>
15. Grompe M, Al-Dhalimy M, Finegold M, Ou CN, Burlingame T, Kennaway NG, Soriano P. Loss of fumarylacetoacetate hydrolase is responsible for the neonatal hepatic dysfunction phenotype of lethal albino mice. *Genes Dev* 1993;7:2298-2307. <https://doi.org/10.1101/gad.7.12a.2298>
16. Wu LL, Wang HY, Chen PJ. Hydrodynamic HBV transfection mouse model. *Methods Mol Biol* 2017;1540:227-235. https://doi.org/10.1007/978-1-4939-6700-1_19
17. Yan Z, Zeng J, Yu Y, Xiang K, Hu H, Zhou X, Gu L, Wang L, Zhao J, Young JAT, Gao L. HBVcircle: A novel tool to investigate hepatitis B virus covalently closed circular DNA. *J Hepatol* 2017;66:1149-1157. <https://doi.org/10.1016/j.jhep.2017.02.004>
18. Ortega-Prieto AM, Cherry C, Gunn H, Dorner M. In vivo model systems for hepatitis B virus research. *ACS Infect Dis* 2019;5:688-702. <https://doi.org/10.1021/acscinfedis.8b00223>
19. Milich DR, Leroux-Roels GG. Immunogenetics of the response to HBsAg vaccination. *Autoimmun Rev* 2003;2:248-257. [https://doi.org/10.1016/S1568-9972\(03\)00031-4](https://doi.org/10.1016/S1568-9972(03)00031-4)
20. Peng XH, Ren XN, Chen LX, Shi BS, Xu CH, Fang Z, Liu X, Chen JL, Zhang XN, Hu YW, Zhou XH. High persistence rate of hepatitis B virus in a hydrodynamic injection-based transfection model in C3H/HeN mice. *World J Gastroenterol* 2015;21:3527-3536. <https://doi.org/10.3748/wjg.v21.i12.3527>
21. Santantonio T, Jung MC, Pastore G, Angarano G, Günther S, Will H. Familial clustering of HBV pre-C and pre-S mutants. *J Hepatol* 1997;26:221-227. [https://doi.org/10.1016/S0168-8278\(97\)80034-7](https://doi.org/10.1016/S0168-8278(97)80034-7)
22. Huang LR, Wu HL, Chen PJ, Chen DS. An immunocompetent mouse model for the tolerance of human chronic hepatitis B virus infection. *Proc Natl Acad Sci U S A* 2006;103:17862-17867. <https://doi.org/10.1073/pnas.0608578103>
23. Wang D, Tai PWL, Gao G. Adeno-associated virus vector as a platform for gene therapy delivery. *Nat Rev Drug Discov* 2019;18:358-378. <https://doi.org/10.1038/s41573-019-0012-9>
24. Guo X, Chen P, Hou X, Xu W, Wang D, Wang TY, Zhang L, Zheng G, Gao ZL, He CY, Zhou B, Chen ZY. The recombinant cccDNA produced using minicircle technology mimicked HBV genome in structure and function closely. *Sci Rep* 2016;6:25552. <https://doi.org/10.1038/srep25552>
25. Wang L, Cao M, Wei QL, Zhao ZH, Xiang Q, Wang HJ, Zhang HT, Lai GQ. A new model mimicking persistent HBV e antigen-negative infection using covalently closed circular DNA in immunocompetent mice. *PLoS One* 2017;12:e0175992. <https://doi.org/10.1371/journal.pone.0175992>
26. Chou HH, Chien WH, Wu LL, Cheng CH, Chung CH, Horng JH, Ni YH, ET AL. Age-related immune clearance of hepatitis B virus infection requires the establishment of gut microbiota. *Proc Natl Acad Sci U S A* 2015;112:2175-2180. <https://doi.org/10.1073/pnas.1424775112>
27. Li L, Li S, Zhou Y, Yang L, Zhou D, Yang Y, Lu M, Yang D, Song J. The dose of HBV genome contained plasmid has a great impact on HBV persistence in hydrodynamic injection mouse model. *Virol J* 2017;14:1-12. <https://doi.org/10.1186/s12985-017-0874-6>
28. Suda T, Liu D. Hydrodynamic delivery. *Adv Genet* 2015;89:89-111. <https://doi.org/10.1016/bs.adgen.2014.10.002>
29. Sun Y, Qi Y, Peng B, Li W. NTCP-reconstituted in vitro HBV infection system. *Methods Mol Biol* 2017;1540:1-14. https://doi.org/10.1007/978-1-4939-6700-1_1
30. Du Y, Broering R, Li X, Zhang X, Liu J, Yang D, Lu M. In vivo mouse models for hepatitis B virus infection and their application. *Front Immunol* 2021;12:4578. <https://doi.org/10.3389/fimmu.2021.766534>
31. Řezáčová P, Pokorná J, Brynda J, Kožíšek M, Cígler P, Lepšík M, Fanfrlík J, ET AL. Design of HIV protease inhibitors based on inorganic polyhedral metallacarboranes. *J Med Chem* 2009;52:7132-7141. <https://doi.org/10.1021/jm9011388>

-
32. Kao JH. Diagnosis of hepatitis B virus infection through serological and virological markers. *Expert Rev Gastroenterol Hepatol* 2008;2:553-562. <https://doi.org/10.1586/17474124.2.4.553>
 33. Kramvis A. Genotypes and genetic variability of hepatitis B virus. *Intervirology* 2014;57:141-150. <https://doi.org/10.1159/000360947>
 34. Sengupta S, Rehman S, Durgapal H, Acharya SK, Panda SK. Role of surface promoter mutations in hepatitis B surface antigen production and secretion in occult hepatitis B virus infection. *J Med Virol* 2007;79:220-228. <https://doi.org/10.1002/jmv.20790>
 35. Zhou T, Guo H, Guo JT, Cuconati A, Mehta A, Block TM. Hepatitis B virus e antigen production is dependent upon covalently closed circular (ccc) DNA in HepAD38 cell cultures and may serve as a cccDNA surrogate in antiviral screening assays. *Antiviral Res* 2006;72:116-124. <https://doi.org/10.1016/j.antiviral.2006.05.006>
 36. Levrero M, Pollicino T, Petersen J, Belloni L, Raimondo G, Dandri M. Control of cccDNA function in hepatitis B virus infection. *J Hepatol* 2009;51:581-592. <https://doi.org/10.1016/j.jhep.2009.05.022>
 37. The World Health Organisation. Guidelines on Hepatitis B and C Testing, 2017.
-